Targeting the unstable atherosclerotic plaque : diagnostic and therapeutic implications

Segers, F.M.E.

Chapter 5

Scavenger Receptor-AI Targeted Contrast Agents Show Improved T2-weighted Magnetic Resonance Imaging Signal in Atherosclerotic Lesions

Filip M.E. Segers[1], Ilze Bot[1], Brigit den Adel[2], Linda M. van der Graaf[2], Walter Gonzalez[3], Isabelle Raynal[3], Louise van der Weerd[2,4], Menno P. de Winther[5], Robert E. Poelmann[2], Theo J.C. van Berkel[1], and Erik A.L. Biessen[1,6]

[1] Division of Biopharmaceutics, Leiden/Amsterdam Center for Drug Research, Leiden University, Leiden, The Netherlands
[2] Department of Anatomy and Embryology, Leiden University Medical Center, Leiden, The Netherlands
[3] Recherche Biologique, Guerbet, Aulnay-sous-bois, France
[4] Department of Radiology, Leiden University Medical Center, Leiden, The Netherlands
[5] Department of Molecular Genetics, Cardiovascular Research Institute Maastricht, Maastricht University, Maastricht, The Netherlands
[6] Department of Pathology, Cardiovascular Research Institute Maastricht, Maastricht University, Maastricht, The Netherlands

(Manuscript in preparation)

ABSTRACT

Background - In search of targeted molecular imaging modalities for specific detection of inflammatory high risk atherosclerotic plaques, we have investigated the imaging potential of scavenger receptor-AI (SR-AI), which is highly expressed by lesional macrophages and linked to an effective internalization machinery.
Methods and Results -Iron-oxide based USPIO were equipped with a peptidic SR-AI ligand (0.371mol Fe/L and 0.018mol PP1/L). Both human and murine macrophages incubated with targeted USPIO had significantly higher iron uptake than non-targeted USPIO as judged from quantitative atomic absorption spectroscopy and Perl's staining. This increment was shown to be strictly mediated via scavenger receptors. Upon injection in ApoE-/- mice targeted USPIO displayed an accelerated plasma decay, and a 3.5 fold increase ($p=0.01$) in atherosclerotic plaque accumulation as compared to non-targeted USPIO. Whole body MRI analysis of atherosclerotic LDLr-/- chimeras with leukocyte expression of human SR-AI versus leukocyte SR-AI deficiency revealed a significant improvement in contrast-to-noise ratio (2.7-fold; $p=0.003$) in atherosclerotic aortic arches in mice or expression of human SR-AI 24h after injection of SR-AI targeted USPIO.
Conclusions - Collectively our data show that SR-AI targeted molecular imaging with a specific phage-display-derived peptide holds great promise for diagnosis of inflammatory plaques in manifest atherosclerosis.

INTRODUCTION

Despite recent advancement in our understanding of the pathogenesis of acute cardiovascular syndromes (ACS), the current diagnostic modalities are primarily appropriate for detecting the degree of stenosis, but lack the desired specificity to identify those atherosclerotic plaques that are at risk of becoming clinically symptomatic. Non-invasive detection methods, such as magnetic resonance imaging (MRI), may enable early tracking of subclinical lesions, characterization of plaque composition and an accurate discrimination between stable and unstable lesions. To augment the inherently low sensitivity of MRI superparamagnetic contrast agents have been developed and are to date widely used as contrast agents for molecular and cellular imaging[1]. An example of such an agent is Ferumoxtran-10, an ultrasmall superparamagnetic iron based oxide nanoparticle (USPIO). USPIOs have already been applied for detection of metastases[2, 3], multiple sclerosis lesions[4, 5], inflammatory foci in the central nervous system[6] and atherosclerotic plaques[7, 8]. USPIO particles are only slowly cleared from the bloodstream, potentially via receptor mediated endocytosis[9] by macrophages, and as a result display a long half life in circulation to end up in lymph node macrophages and peripheral tissue macrophages[10, 11]. Nevertheless, plaque uptake is rather inefficient, possibly due to its low affinity for the major elimination receptors. USPIO were reported to reside in the lysosomal compartment for up to 7 days in vitro[12] before complete degradation. The dextran coating is progressively degraded and almost exclusively eliminated via the urinary system, whereas iron is assimilated in the body's iron pool, progressively incorporated in red bood cells (haemoglobin) and finally eliminated via faeces after 84 days[1]. While advantageous for some imaging purposes a prolonged biological half-life may be accompanied by cytotoxic effects on the long run[13].

A hallmark in the pathogenesis of atherosclerosis is monocyte infiltration, their differentiation into macrophages and foam cells and subsequent activation in the arterial intima[14]. Plaque macrophages highly express class A scavenger receptors (SR-A), which have been suggested to play a crucial role in atherosclerotic lesion development[15-18]. Scavenger receptor-mediated uptake of modified lipoproteins is deemed instrumental in foam cell formation and activation, promoting a pro-inflammatory phenotype of lesional macrophages[19]. Abundant scavenger receptor expression was found in lesion-specific foam cells and vascular smooth muscle cells but not in the healthy vessel wall[20, 21]. Relevant to vulnerable plaque detection abundant SR-AI expression was shown in macrophage enriched inflammatory foci in the advanced, atherosclerotic lesion. Combined with efficient receptor-mediated endocytosis of bound substrates this qualifies SR-AI as promising target for plaque-directed molecular imaging and drug delivery approaches. Due to the complex chemical nature of known macromolecular SR-AI substrates, attempts in ligand design for this receptor have so far been rather unsuccessful. We have recently identified a 15-mer peptide PP1 by phage display library screening, which

shows high *in vitro* and *in vivo* affinity and specificity for both human and murine macrophage scavenger receptor class A[22].
In our current study we describe the development and potential of SR-AI targeted USPIO particles functionalized with the SR-A specific peptide. The targeted USPIO displayed a decreased blood half life and a concomitant increase in lesional macrophage uptake. The latter resulted in enhanced MRI signal in macrophages *in vitro* and *in vivo* in atherosclerotic plaques.

MATERIALS AND METHODS

Cell culture

RAW264.7 murine macrophage cells and human THP-1 monocyte cells (gift from Guerbet Group) were grown at 37°C in a humidified atmosphere (5% CO_2) in Dulbecco's Modified Eagle's Medium (DMEM) and RPMI 1640 medium, respectively, supplemented with 10% Fetal Bovine Serum (FBS) (Heat-inactivated, 30min 56°C), 2mmol/L L-glutamine, 100 U/ml Penicillin and 100µg/ml streptomycin (all from PAA, Cölbe, Germany). THP-1 monocytes were differentiated into macrophages by incubating the cells with phorbol 12-myristate, 13-acetate (PMA, 100nM, o.n.) (Sigma, Zwijndrecht, The Netherlands). Fucoidan (Sigma, Zwijndrecht, The Netherlands) was used as an inhibitor for SR-AI.

Animals

All animal work was performed in compliance with the Dutch government guidelines. ApoE$^{-/-}$ (1-year old) and female LDLr$^{-/-}$ mice (aged 8-12 weeks) were obtained from the local animal breeding facility. SR-A1$^{-/-}$ mice were from Jacksons Laboratory (Bar Harbor, Maine, USA) and transgenic mice with human SR-A overexpression on a SR-AI deficient background were obtained from Dr. Menno de Winther, Maastricht University Medical Center, the Netherlands. All mice were kept under standard laboratory conditions. Diet and water were provided *ad libitum* throughout the experiment.

Bone Marrow Transplantation and induction of hypercholesterolemia

Female LDLr$^{-/-}$ mice were lethally irradiated by a single dose of 9 Gy (0.19 Gy/min, 200 kV, 4 mA) total body irradiation, using an Andrex Smart 225 Röntgen source (YXLON Int, Copenhagen, Denmark) equipped with a 6-mm aluminium filter. Bone marrow was isolated by flushing the femurs and tibias from donor mice with phosphate-buffered saline (PBS). Single-cell suspensions were prepared by passing the cells through a 30-µm nylon gauze. Irradiated recipients received $0.5x10^7$ bone marrow cells by intravenous injection into the tail vein. After a recovery of 6 weeks animals received a semisynthetic high-cholesterol diet containing 15% (w/w) fat and 0.25% (w/w) cholesterol (Diet W; Abdiets, Woerden, The Netherlands) for 12-18 weeks. Drinking water was supplied with antibiotics (83 mg/L ciprofloxacin and 67 mg/L polymyxin B sulfate) and 6.5 g/L sucrose. Mouse health and weight was monitored during the experiment and blood samples were collected by tail bleeding every 2-3 weeks for assessment of plasma cholesterol

levels. Total cholesterol levels were quantified spectrophotometrically using an enzymatic procedure (Roche Diagnostics, Germany). Precipath standardized serum (Boehringer, Germany) was used as an internal standard.

MRI

All experiments were performed on a 9.4T (400 MHz) vertical 89-mm bore MR magnet interfaced to a Bruker AVANCE (Bruker BioSpin MRI GmbH, Ettlingen, Germany) MR imaging console equipped with ParaVision 5.0 software, with an actively shielded Micro2.5 gradient system (1 T/m). Mice were scanned in a transmit/receive birdcage radiofrequency coil with an inner diameter of 3.0 cm (Bruker BioSpin MRI GmbH, Ettlingen, Germany).

In vivo MRI analysis

In vivo MR imaging analysis was performed on the animals described above ($ApoE^{-/-}$ and bone marrow transplanted $LDLr^{-/-}$ mice). Mice were randomly divided into two groups injected with targeted or non-targeted contrast agent (250µmol Fe/kg). 24h after USPIO injection, mice were anesthetized with isoflurane (2% in air). During the examination the respiration rate was continuously measured with a balloon pressure sensor using a respiration cushion under the mouse chest connected to the ECG/respiratory unit (SA Instruments, Inc., Stony Brook, NY). The isoflurane concentration was adjusted to keep the respiration rate between 50 and 80 respirations/min.

At the start of each examination, several 2D FLASH scout images were recorded in the transverse and axial plane of the heart to determine the orientation of the aortic arch. The following parameters were used for the shout scans: Hermite-shaped RF pulse 1.000 ms; flip angle (FA) 10; repetition time (TR) 14.7 ms; echo time (TE) 1.8 ms; sample rate 40 kHz; echo position 30%; field of view (FOV) 1.8*1.8 cm2 ; matrix 128*128; in-plane resolution 0.141 mm; slice thickness 0.4 mm; number of repetitions 64; total acquisition time approximately 2 min

A modified FLASH sequence with a navigator echo (IntraGate) was used for retrospective CINE MRI with the following parameters:

Hermite-shaped RF pulse 1.000 ms; FA 15°; TR 15.7 ms; TE 2.96 ms; sample rate 40 kHz; echo position 30%; navigator echo points 64; 10 cardiac frames; FOV 2.56*2.56 cm2 ; matrix 128*128; in-plane resolution 0.200 mm; slice thickness 0.5 mm;

number of repetitions 400; total acquisition time approximately 14 min

Image Analysis

For each time point, bright blood images were selected and 3 to 4 adjacent slices of cross-sections of the aortic arch were manually segmented (ImageJ) and contrast-to-noise ratios were determined.

Images were analyzed using ImageJ software. Regions of Interest (ROIs) were drawn around the vessel wall (Iwall). A 2nd ROI was drawn in the muscle tissue of the shoulder region (Imuscle). Furthermore, an ROI was placed outside the animal to measure the noise level (stdevnoise).

Histology and Morphometry

Cryostat sections (10µm) were prepared of the aortic valve area and lipid deposits stained with Oil Red O. Mean lesion area was calculated from 8-10 consecutive Oil Red O (ORO) stained sections. Lesional macrophage content was determined after immunohistochemical staining with a macrophage specific antigen antibody (MoMa-2, monoclonal rat IgGb2, dilution 1:50; Serotec, Oxford, UK). Secondary antibody goat anti rat IgG-AP (1:100; Sigma, St-Louis, MO) and enzyme substrate Nitro Blue Tetrazolium – 5-Bromo-4-Chloro-3-Idolyl Phospate (NBT-BCIP) (Dako, Glostrup, Denmark) were used. Iron deposits were visualized by hemosiderin staining according to the Perl's method.

Morphometric analysis on Oil Red O and MoMa-2 stained sections was performed using Leica Qwin image analysis software and a Leica-DM-RE microscope (Leica imaging systems, Cambridge, UK). Perl's positive cells were counted manually and in a blinded manner.

Quantitative analysis of iron dosages in plasma and organs

Blood samples were collected by tail vein puncture and plasma was isolated. Upon sacrifice, mice were anesthetized and underwent *in situ* PBS perfusion via the left cardiac ventricle. Organs of interest were isolated and stored at -80°C until further analysis. Iron content of cell cultures and tissue was determined by inductively coupled plasma atomic emission spectroscopy (ICP-AES) (Optima 3300 RL, Perkin Elmer, Courtaboeuf, France)

RESULTS

Increased uptake of scavenger receptor targeted USPIO by macrophages in vitro

The kinetics of uptake, processing and detection of USPIO *in vitro* and *in vivo*[9] have been subject of numerous studies. Here we sought to investigate whether USPIO could be rendered plaque specific by conjugation of a newly devised peptide ligand for SR-AI, a receptor that was previously shown to be highly expressed by macrophages and inflammatory foci within the plaque[23].

Quantitative atomic absorption spectroscopy analysis showed a significant increase in iron uptake in RAW264.7 cells incubated with targeted (T-USPIO) versus that in non-targeted USPIO (300µg Fe/ml) (1729 ± 152 to 805 ± 111ng Fe/g cell pellet, $p<0.001$, figure 5.1A). Similar in vitro uptake studies in human THP-1 macrophages revealed a comparably, significant increased cellular uptake of T-USPIO (600 ± 35) over USPIO (343 ± 48 ng Fe/g cell pellet, $p=0.01$). T-USPIO uptake could be blocked by pre-incubation of the cells with fucoidan, an established inhibitor of SR-AI/II[24] (figure 5.1B).

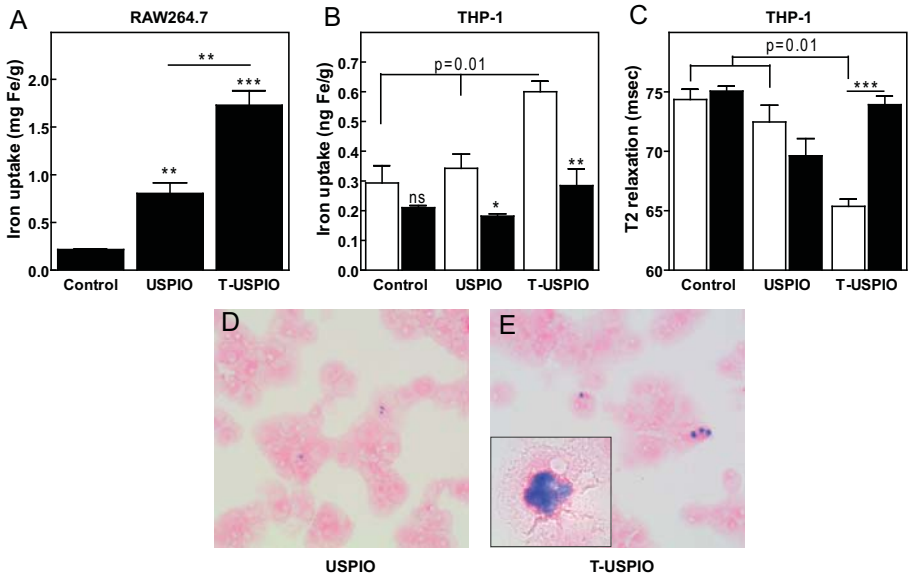

Figure 5.1 Scavenger receptor targeted USPIO display improved uptake by macrophages in vitro compared to untargeted USPIO. Cellular uptake of targeted (T-USPIO; 300µg Fe/ml) and non-targeted USPIO (USPIO, 300µg Fe/ml) was assessed in different *in vitro* macrophage cell cultures. Cells without contrast agents served as control. (A) RAW264.7 macrophages were incubated with T-USPIO or USPIO for 24h. Cell pellets were collected and quantitatively analyzed by inductively coupled plasma atomic emission spectroscopy (ICP-AES). (B) THP-1 macrophages with (white) or without (black) inhibitor (Fucoidan; 0.5mg/ml) were incubated for 24h with USPIO and T-USPIO. Uptake of (T-)USPIO was determined by ICP-AES based iron analysis of cell lysates and corrected for protein content. (C) T2 relaxation times from these cell pellets were also analyzed by MRI. Iron uptake was reflected by signal loss in T_2-weighted MRI analysis of cell pellets. THP-1 incubated with USPIO (D) and T-USPIO (E) were stained for iron with Perl's staining to visualize intracellular iron deposition. Data are shown as mean ± SEM. (**p<0.05, **p<0.01 and ***p<0.001)*

The increased T-USPIO uptake by THP-1 cells is accompanied by an improved MRI signal, as judged by shorter T_2 relaxation times in cells incubated T-USPIO (65.4 ± 0.6 msec; p=0.01) compared to its non-targeted counterpart (72.5 ±1.4msec) (Figure 5.1C). Again, incubation with fucoidan blunted the decrease in T2 relaxation of T-USPIO, but to a lesser extent also of USPIO incubated macrophages, which is compatible with the previously suggested role of scavenger receptors in USPIO uptake. In fact, T2 relaxation times after fucoidan treatment were comparable to that of the control samples.
In keeping with these in vitro MRI data, Perl's staining of THP-1 macrophages confirmed a more abundant presence of intracellular hemosiderin deposits in T-USPIO incubated macrophages (figure 5.1D-E) . These results clearly indicate that targeting USPIO particles leads to a significantly increased and SR-AI dependent uptake by macrophages in vitro.

Increased plasma clearance and increased signal in vivo upon targeted delivery of USPIO in ApoE$^{-/-}$ mice

As a next step, we investigated plaque accumulation of the SR-AI targeted T-UPSIO particles *in vivo* in 1-year old ApoE$^{-/-}$ mice (N=14) with established advanced atherosclerotic lesions. A subset of mice received a single intravenous injection with T-USPIO (250µmol Fe/kg, N=6) and another group received its non-targeted counterpart (250µgmol Fe/kg, N=6). The remaining mice were used to determine endogenous tissue iron content. Kinetic analysis of plasma iron levels by ICP-AES pointed to an increased plasma clearance of T-USPIO ($T_{1/2}$ = 1.7h) compared to the untargeted contrast agent (T1/2 = 2.9h; P<0.05). For both contrast agents baseline levels of plasma iron were reached within 24h after administration (figure 5.2A).

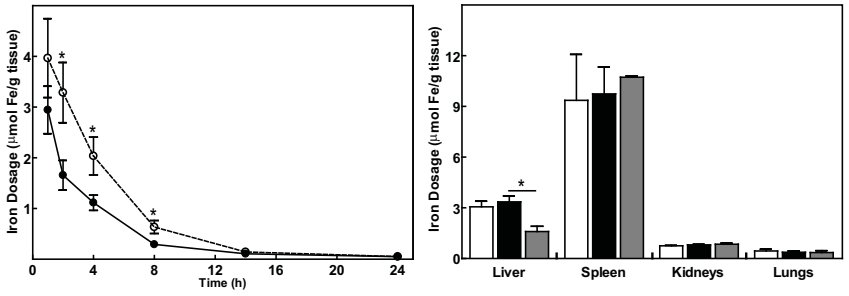

Figure 5.2 Targeted USPIO show faster kinetics in blood and improved accumulation in macrophage-rich organs. Aged ApoE$^{-/-}$ (1-year old) mice received USPIO (N=6) or targeted USPIO (T-USPIO; N=6) (250umol Fe/kg) by intravenous injection. Mock injected mice served as control and were used to determine endogenous tissue iron concentrations. Blood samples were collected at 1, 2, 4, 8, 14h and 24h (point of sacrifice). Plasma samples were subjected to ICP-AES atomic absorption spectroscopy and iron content in mice treated with T-USPIO (●) and untargeted USPIO (O) was determined (A). At 24h after administration, organs of interest were harvested and analyzed for iron uptake by ICP-AES (B). The results for the non-targeted USPIO group are shown in white bars, while those for T-USPIO are indicated in black. Grey bars represent endogenous tissue iron contents from control mice. Data are shown as mean ± SEM. (**p<0.05*)

Analysis of macrophage-rich organs such as liver, spleen and lungs as well as kidney for iron content 24h after injection, showed increased iron accumulation in liver, the primary target organ, in USPIO and even more so in T-USPIO treated mice (3355 ± 355nmol Fe/g tissue; $p<0.05$) versus non-treated controls (1599 ± 313nmol Fe/g). The biodistribution profiles of T-USPIO and USPIO were rather similar and did not significantly differ from that of the untreated controls (Figure 5.2B). Lesion prone artery segments (aortic valve area, figure 5.3) were also analyzed for lesion size, monocyte/macrophage content and iron accumulation. As expected no differences were observed in lesion size (figure 5.3A-C) and monocyte/macrophage content at 24h after administration (figure 5.3 D-F). However visualization of iron uptake by Perl's staining revealed a significant, 3.3-fold increase in Perl's positive cells in lesions of T-USPIO injected mice compared to that treated with USPIO ($P=0.01$). Our data thus demonstrate that targeted contrast agents combine accelerated plasma clearance with increased accumulation in advanced atherosclerotic lesions.

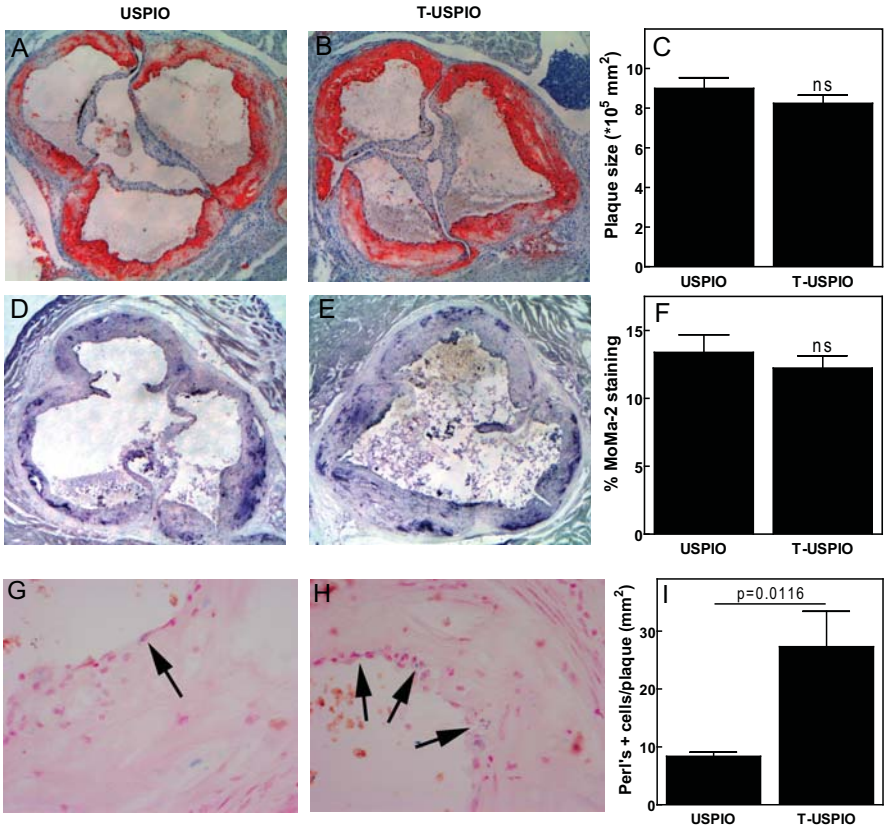

Figure 5.3 SR-AI targeting of contrast agents results in increased uptake in advanced atherosclerotic plaques in ApoE$^{-/-}$ mice. Aged ApoE$^{-/-}$ (1-year old) mice received an intravenous injection of non-targeted (USPIO; 250µmol Fe/kg; N=6) or targeted USPIO (T-USPIO; 250µmol Fe/kg; N=6). After 24h mice were sacrificed and sections were made of the atherosclerotic lesion prone aortic root. These sections were subsequently stained for Perl's (G-H), Oil-Red-O (A-C), and MoMa-2 (D-F). Plaque size (C) and macrophage content (F) were determined with computer assisted image analysis. (I)Perl's stained sections were analyzed in a blinded manner and Perl's stained cells were individually scored (data presented as # Perl's positive cells/plaque area). Data are shown as mean ± SEM.

T-USPIO show superior accumulation in plaques in a humanized mouse model of atherosclerosis

In initial studies we showed that the SR-AI targeting peptide PP1[25] had even higher affinity for human derived THP-1 macrophages than for murine macrophages, suggesting that PP1 may be at least equally effective in targeting human plaques. To address its potential for human plaque imaging we have generated LDLr$^{-/-}$ chimeras with hematopoietic human SR-AI expression by bone marrow transplantation. Chimeras with hematopoietic SR-AI deficiency served as control. After a recovery period of 6 weeks, atherogenesis was induced by high cholesterol diet feeding. Both groups of mice received a single intravenous dose of PP1-targeted contrast agent (T-USPIO; 250µmol Fe/kg). 24h later mice were anesthetized and subjected to *in vivo* magnetic resonance imaging on a 9.4 Tesla MRI apparatus. In keeping with previous findings[26, 27] morphometric analysis did not reveal any differences in plaque size between SR-AI$^{-/-}$ and hSR-AI mice (figure 5.4A-C). Importantly, plaque monocyte/macrophage content of the atherosclerotic lesions did also not differ (figure 5.4D-F). *In vivo* MRI analysis of the aortic arch revealed a significantly decreased in signal-to-noise ratio in mice overexpressing hSR-A (-17.4 ± 2.3) compared to SR-A$^{-/-}$ controls (-6.4 ± 0.5; p=0.004) (figure 5.5). The signal loss in T2 weighted analysis pointed to an augmented iron uptake in hSR-A overexpressing mice. These results clearly illustrate the improved capacity of SR-AI targeted contrast agents to accumulate in atherosclerotic lesions in a SR-AI dependent manner.

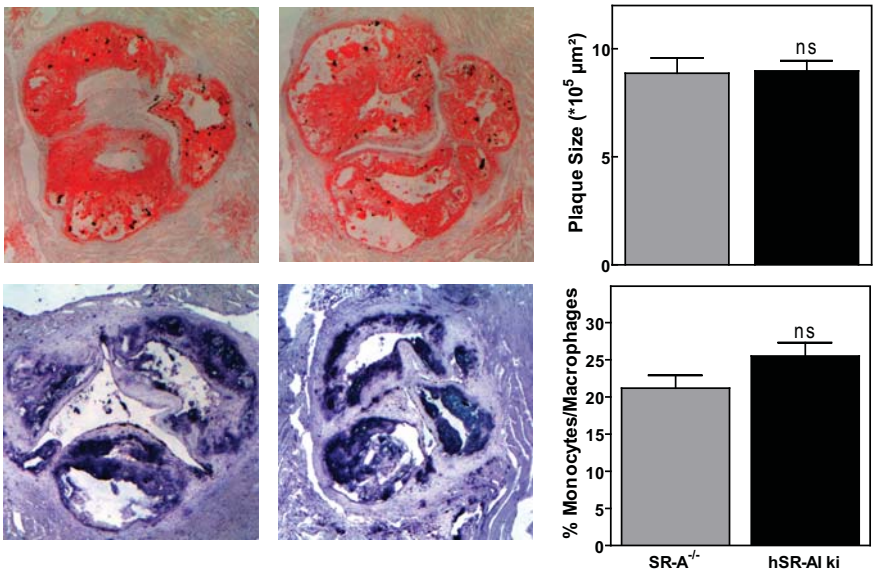

Figure 5.4 LDLr$^{-/-}$ chimeras with hematopoietic SR-A deficiency (SR-AI$^{-/-}$) or hSR-AI overexpression (hSRAI) have similar plaque size and composition. After bone marrow transplantation, LDLr$^{-/-}$ chimeras with hematopoietic SR-A$^{-/-}$ (gray bars) and hSR-A overexpression (black bars), were fed a high cholesterol diet to induce atherosclerotic plaque formation. Both groups received a single injection of T-USPIO (250µmol Fe/kg) and 24h later mice were sacrificed, and aortas were excised. Cryosections were made from the atherosclerotic lesion prone aortic root and subsequently stained for Oil-Red-O (A-B) and MoMa-2 (D-E). Plaque size (C) and macrophage content (F) were determined with computer assisted image analysis. Data are shown as mean ± SEM.

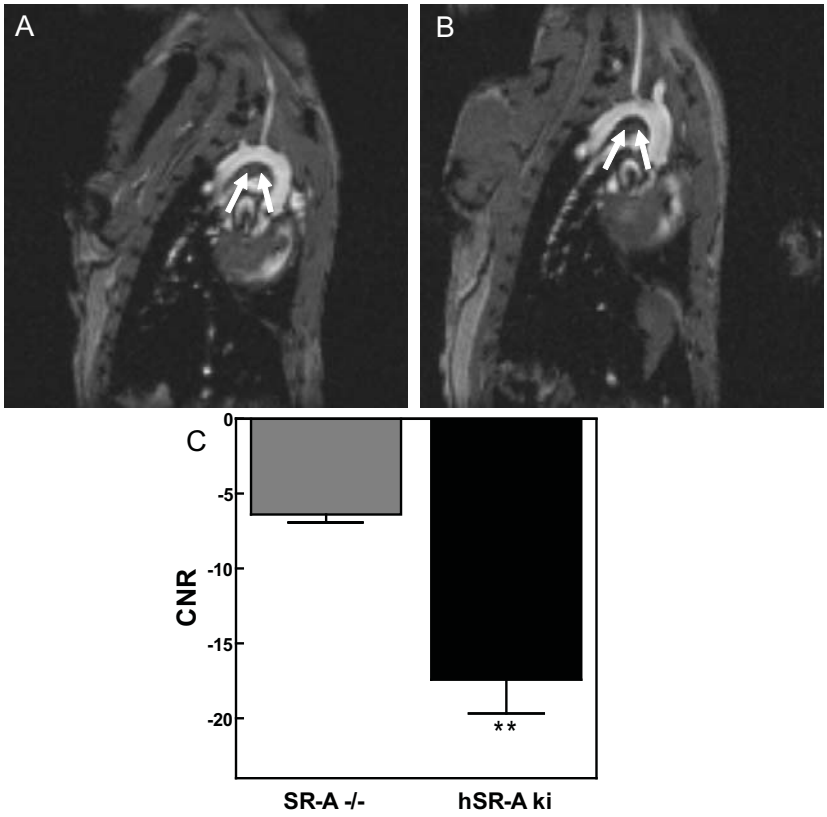

Figure 5.5 ***In vivo*** **Magnetic Resonance Imaging of the aortic arch reveals increased lesional uptake of targeted USPIO in hSR-A overexpressing LDLr$^{-/-}$ chimeras.** After bone marrow transplantation, LDLr$^{-/-}$ chimeras were fed a high cholesterol diet to induce atherosclerotic plaque formation. SR-A$^{-/-}$ (N=4, gray bars) and hSR-A overexpressing (N=6, black bars) bone marrow recipients received a single administration with targeted USPIO (250 µmol Fe/kg). At 24h after injection, mice were subjected to in vivo magnetic resonance imaging and subsequently sacrificed. Contrast-to-Noise Ratio (CNR) was determined by computer assisted analysis of MRI images (A-B). For each mouse three images were analyzed and mean CNR was determined (C). Data are shown as mean ± SEM. ***(**p<0.01)***

DISCUSSION

Ultrasmall superparamagnetic iron oxide particles (USPIO) are widely used in non-invasive clinical imaging to enhance image contrast in detection of malignancies[28], inflammatory multiple sclerosis lesions, CNS pathologies and atherosclerotic lesions[7]. One of the major challenges in cardiovascular imaging is the clinically relevant distinction between stable and unstable rupture-prone lesions. The latter are typified by the abundant presence of leukocytes such as macrophages, which play a central role in plaque destabilization[29]. This renders macrophages primary targets in diagnostic strategies for vulnerable plaque detection. An interesting candidate in this regard might be scavenger receptor AI, which is highly expressed on plaque macrophages and efficiently conveys substrates to the endocytotic compartment[15, 30, 31]. Our group recently successfully identified a small 15-mer peptide (PP1) with high specificity and affinity for scavenger receptor class AI[22]. Here we describe the conjugation of PP1 to USPIO particles and we not only show induced delivery of this PP1 conjugated USPIO to macrophages *in vitro* and *in vivo* but also enhanced MRI image contrast in macrophage rich atherosclerotic plaques in a humanized model of atherosclerosis.

In the first step we developed a targeted USPIO coated on its outer layer with PP1 peptide (5%; 0.018mol PP1/L and 0.371mol Fe/L), from here on referred to as T-USPIO. Our results show increased *in vitro* uptake of T-USPIO in murine (2.1-fold) and human macrophages (1.8 fold) compared to its untargeted counterpart. The induced uptake was almost completely blunted by a SR-AI antagonist, fucoidan. Combined these data confirm that like PP1 itself, PP1 targeted UPSIO are preferentially taken up by macrophages via a scavenger-receptor mediated pathway as well. Interestingly, even uptake of conventional USPIO by macrophages was partly inhibited by fucoidan, which is in keeping with previous studies that implicated scavenger receptor class A in USPIO uptake[9]. Clearly however, macrophage accumulation of T-USPIO *in vitro* is more efficient than of untargeted USPIO.

The *in vitro* data on increased accumulation of T-USPIO were confirmed *in vivo*. *In vivo* accumulation of the targeted contrast agent was tested after intravenous administration in aged ApoE$^{-/-}$ mice with advanced atherosclerotic lesions. As shown previously, these mice express high levels of scavenger receptor on lesion macrophages (Molenaar et al. personal communication). T-USPIO had faster plasma decay and increased hepatic uptake than USPIO. Iron accumulation in other organs was not notably altered by SR-AI targeting. The biodistribution profile of T-USPIO was consistent with that of [^{125}I]-labeled PP1[22]. T-USPIO and USPIO both were almost completely cleared from plasma within 24 hours after administration. The accelerated decay and targeted tissue uptake leads to faster normalization of blood signal intensity, which is beneficial for vessel wall analysis. In addition, it reduces nonspecific USPIO accumulation in surrounding tissue which further increases signal-to-noise ratio in the vessel wall. Furthermore fast

plasma clearance will minimize the risk of USPIO associated systemic toxicity. Importantly, accelerated elimination kinetics of T-USPIO led to preferential accumulation in advanced atherosclerotic lesions as compared to non-targeted USPIO. The increased uptake was not attributable to differences in lesion size or characteristics, suggesting that it is directly related to increased uptake of these particles by SR-AI expressing plaque macrophages.

In a next experiment we aimed to extend these findings to a second, humanized model of atherosclerosis, LDLr$^{-/-}$ chimeras with macrophage expression of human SR-A. We generated LDLr$^{-/-}$ mice with macrophage-specific overexpression the human macrophage scavenger receptor class A[27, 32] or with leukocyte SR-AI deficiency[26]. *In vivo* MRI image analysis demonstrated increased uptake of T-USPIO in plaques of mice expressing human SR-A[33]. Again neither plaque size nor macrophage content differed between groups.

Several reports have been published on targeted imaging of inflammation and of vulnerable atherosclerotic plaques. Macrophages remain an important target for imaging as they are inflammatory key effectors in atherosclerosis[29] and high abundance in plaque was seen to associate with a high risk of clinical complications[34-36]. Currently two major approaches exist for imaging intraplaque macrophage density. Macrophages have been targeted in a passive manner, either directly after penetration of USPIO into the plaque and ingestion in situ, or directly after USPIO uptake by monocytes and their subsequent migration into the atherosclerotic plaque[37]. Alternatively, active targeting of intraplaque macrophages has been employed using Gd-based micelles that were linked to a specific homing device (antibody) against SR-AI/II[38]. Next to macrophages, a variety of vulnerable plaque components or processes have been considered for targeted plaque imaging, including apoptosis[39], necrosis[39], neovascularization, modified LDL[40, 41] extracellular matrix and MMP's have been targeted using Gd-based MR molecular imaging agents[42]. Thus our study provides the first report on molecular imaging using a targeted, USPIO-based contrast agent, which shows high affinity and specificity for murine and human variants of scavenger receptor, which are increased expressed on macrophages in vulnerable atherosclerotic plaquIn conclusion, in our study we successfully developed an SR-AI targeted iron-oxide-based contrast agent that shows increased and SR-AI dependent uptake by macrophages in vitro as well as in vivo in atherosclerotic mouse models. SR-AI targeted contrast agents have a rapid blood decay, and due to their high affinity for SR-AI, this leads to effective, scavenger receptor-AI mediated uptake by atherosclerotic plaque-associated macrophages. As a result they display a favorable signal-to-noise ratio in MRI aided detection of atherosclerotic plaques in a humanized model of atherosclerosis. With these features this targeted contrast agent using a specific SR-A peptide constitutes a promising new platform for the non-invasive detection of macrophage-rich foci in chronic inflammatory diseases such as the atherosclerotic plaque and might even allow selective discrimination of unstable plaques.

REFERENCES

1. Corot C, Robert P, Idee JM, Port M. Recent advances in iron oxide nanocrystal technology for medical imaging. Adv Drug Deliv Rev. 2006;58:1471-1504.
2. Anzai Y, Piccoli CW, Outwater EK, Stanford W, Bluemke DA, Nurenberg P, Saini S, Maravilla KR, Feldman DE, Schmiedl UP, Brunberg JA, Francis IR, Harms SE, Som PM, Tempany CM. Evaluation of neck and body metastases to nodes with ferumoxtran 10-enhanced MR imaging: phase III safety and efficacy study. Radiology. 2003;228:777-788.
3. Harisinghani MG, Barentsz J, Hahn PF, Deserno WM, Tabatabaei S, van de Kaa CH, de la Rosette J, Weissleder R. Noninvasive detection of clinically occult lymph-node metastases in prostate cancer. N Engl J Med. 2003;348:2491-2499.
4. Rausch M, Hiestand P, Baumann D, Cannet C, Rudin M. MRI-based monitoring of inflammation and tissue damage in acute and chronic relapsing EAE. Magn Reson Med. 2003;50:309-314.
5. Rausch M, Hiestand P, Foster CA, Baumann DR, Cannet C, Rudin M. Predictability of FTY720 efficacy in experimental autoimmune encephalomyelitis by in vivo macrophage tracking: clinical implications for ultrasmall superparamagnetic iron oxide-enhanced magnetic resonance imaging. J Magn Reson Imaging. 2004;20:16-24.
6. Pirko I, Johnson A, Ciric B, Gamez J, Macura SI, Pease LR, Rodriguez M. In vivo magnetic resonance imaging of immune cells in the central nervous system with superparamagnetic antibodies. FASEB J. 2004;18:179-182.
7. Corot C, Petry KG, Trivedi R, Saleh A, Jonkmanns C, Le Bas JF, Blezer E, Rausch M, Brochet B, Foster-Gareau P, Baleriaux D, Gaillard S, Dousset V. Macrophage imaging in central nervous system and in carotid atherosclerotic plaque using ultrasmall superparamagnetic iron oxide in magnetic resonance imaging. Invest Radiol. 2004;39:619-625.
8. Kooi ME, Cappendijk VC, Cleutjens KB, Kessels AG, Kitslaar PJ, Borgers M, Frederik PM, Daemen MJ, van Engelshoven JM. Accumulation of ultrasmall superparamagnetic particles of iron oxide in human atherosclerotic plaques can be detected by in vivo magnetic resonance imaging. Circulation. 2003;107:2453-2458.
9. Raynal I, Prigent P, Peyramaure S, Najid A, Rebuzzi C, Corot C. Macrophage endocytosis of superparamagnetic iron oxide nanoparticles: mechanisms and comparison of ferumoxides and ferumoxtran-10. Invest Radiol. 2004;39:56-63.
10. Weissleder R, Elizondo G, Wittenberg J, Rabito CA, Bengele HH, Josephson L. Ultrasmall superparamagnetic iron oxide: characterization of a new class of contrast agents for MR imaging. Radiology. 1990;175:489-493.
11. Bourrinet P, Bengele HH, Bonnemain B, Dencausse A, Idee JM, Jacobs PM, Lewis JM. Preclinical safety and pharmacokinetic profile of ferumoxtran-10, an ultrasmall superparamagnetic iron oxide magnetic resonance contrast agent. Invest Radiol. 2006;41:313-324.
12. Schulze E, Ferrucci JT, Jr., Poss K, Lapointe L, Bogdanova A, Weissleder R. Cellular uptake and trafficking of a prototypical magnetic iron oxide label in vitro. Invest Radiol. 1995;30:604-610.
13. Muller K, Skepper JN, Posfai M, Trivedi R, Howarth S, Corot C, Lancelot E, Thompson PW, Brown AP, Gillard JH. Effect of ultrasmall superparamagnetic iron oxide nanoparticles (Ferumoxtran-10) on human monocyte-macrophages in vitro. Biomaterials. 2007;28:1629-1642.
14. Ross R. Atherosclerosis--an inflammatory disease. N Engl J Med. 1999;340:115-126.
15. Hiltunen TP, Luoma JS, Nikkari T, Yla-Herttuala S. Expression of LDL receptor, VLDL receptor, LDL receptor-related protein, and scavenger receptor in rabbit atherosclerotic lesions: marked induction of scavenger receptor and VLDL receptor expression during lesion development. Circulation. 1998;97:1079-1086.
16. Kunjathoor VV, Febbraio M, Podrez EA, Moore KJ, Andersson L, Koehn S, Rhee JS, Silverstein R, Hoff HF, Freeman MW. Scavenger receptors class A-I/II and CD36 are the principal receptors responsible for the uptake of modified low density lipoprotein leading to lipid loading in macrophages. J Biol Chem. 2002;277:49982-49988.
17. van Berkel TJ, Out R, Hoekstra M, Kuiper J, Biessen E, van Eck M. Scavenger receptors: friend or foe in atherosclerosis? Curr Opin Lipidol. 2005;16:525-535.

18. Suzuki H, Kurihara Y, Takeya M, Kamada N, Kataoka M, Jishage K, Ueda O, Sakaguchi H, Higashi T, Suzuki T, Takashima Y, Kawabe Y, Cynshi O, Wada Y, Honda M, Kurihara H, Aburatani H, Doi T, Matsumoto A, Azuma S, Noda T, Toyoda Y, Itakura H, Yazaki Y, Kodama T, et al. A role for macrophage scavenger receptors in atherosclerosis and susceptibility to infection. Nature. 1997;386:292-296.

19. Moore KJ, Freeman MW. Scavenger receptors in atherosclerosis: beyond lipid uptake. Arterioscler Thromb Vasc Biol. 2006;26:1702-1711.

20. Gough PJ, Greaves DR, Suzuki H, Hakkinen T, Hiltunen MO, Turunen M, Herttuala SY, Kodama T, Gordon S. Analysis of macrophage scavenger receptor (SR-A) expression in human aortic atherosclerotic lesions. Arterioscler Thromb Vasc Biol. 1999;19:461-471.

21. de Winther MP, van Dijk KW, Havekes LM, Hofker MH. Macrophage scavenger receptor class A: A multifunctional receptor in atherosclerosis. Arterioscler Thromb Vasc Biol. 2000;20:290-297.

22. Segers FME YH, Molenaar TJM, Prince P, Tanaka T, van Berkel TJ, and Biessen EAL. Identification of a Novel Peptide Antagonist of SR-AI as Atherosclerosis-targeted Imaging Agent.

23. Matsumoto A, Naito M, Itakura H, Ikemoto S, Asaoka H, Hayakawa I, Kanamori H, Aburatani H, Takaku F, Suzuki H, et al. Human macrophage scavenger receptors: primary structure, expression, and localization in atherosclerotic lesions. Proc Natl Acad Sci U S A. 1990;87:9133-9137.

24. Platt N, Gordon S. Scavenger receptors: diverse activities and promiscuous binding of polyanionic ligands. Chem Biol. 1998;5:R193-203.

25. Segers FME YH, Molenaar TJM, Prince P, Tanaka T, van Berkel TJ, and Biessen EAL. Identification of a Novel Peptide Antagonist of SR-AI as Atherosclerosis-targeted Imaging Agent; 2010.

26. de Winther MP, Gijbels MJ, van Dijk KW, van Gorp PJ, suzuki H, Kodama T, Frants RR, Havekes LM, Hofker MH. Scavenger receptor deficiency leads to more complex atherosclerotic lesions in APOE3Leiden transgenic mice. Atherosclerosis. 1999;144:315-321.

27. Van Eck M, De Winther MP, Herijgers N, Havekes LM, Hofker MH, Groot PH, Van Berkel TJ. Effect of human scavenger receptor class A overexpression in bone marrow-derived cells on cholesterol levels and atherosclerosis in ApoE-deficient mice. Arterioscler Thromb Vasc Biol. 2000;20:2600-2606.

28. Islam T, Josephson L. Current state and future applications of active targeting in malignancies using superparamagnetic iron oxide nanoparticles. Cancer Biomark. 2009;5:99-107.

29. Libby P. Inflammation in atherosclerosis. Nature. 2002;420:868-874.

30. Yla-Herttuala S, Rosenfeld ME, Parthasarathy S, Sigal E, Sarkioja T, Witztum JL, Steinberg D. Gene expression in macrophage-rich human atherosclerotic lesions. 15-lipoxygenase and acetyl low density lipoprotein receptor messenger RNA colocalize with oxidation specific lipid-protein adducts. J Clin Invest. 1991;87:1146-1152.

31. Hiltunen TP, Yla-Herttuala S. Expression of lipoprotein receptors in atherosclerotic lesions. Atherosclerosis. 1998;137 Suppl:S81-88.

32. de Winther MP, van Dijk KW, van Vlijmen BJ, Gijbels MJ, Heus JJ, Wijers ER, van den Bos AC, Breuer M, Frants RR, Havekes LM, Hofker MH. Macrophage specific overexpression of the human macrophage scavenger receptor in transgenic mice, using a 180-kb yeast artificial chromosome, leads to enhanced foam cell formation of isolated peritoneal macrophages. Atherosclerosis. 1999;147:339-347.

33. Oswald P, Clement O, Chambon C, Schouman-Claeys E, Frija G. Liver positive enhancement after injection of superparamagnetic nanoparticles: respective role of circulating and uptaken particles. Magn Reson Imaging. 1997;15:1025-1031.

34. Choudhury RP, Fuster V, Fayad ZA. Molecular, cellular and functional imaging of atherothrombosis. Nat Rev Drug Discov. 2004;3:913-925.

35. Jaffer FA, Weissleder R. Seeing within: molecular imaging of the cardiovascular system. Circ Res. 2004;94:433-445.

36. Jaffer FA, Libby P, Weissleder R. Molecular and cellular imaging of atherosclerosis: emerging applications. J Am Coll Cardiol. 2006;47:1328-1338.

37. Tang TY, Muller KH, Graves MJ, Li ZY, Walsh SR, Young V, Sadat U, Howarth SP, Gillard JH. Iron oxide particles for atheroma imaging. Arterioscler Thromb Vasc Biol. 2009;29:1001-1008.

38. Lipinski MJ, Amirbekian V, Frias JC, Aguinaldo JG, Mani V, Briley-Saebo KC, Fuster V, Fallon JT, Fisher EA, Fayad ZA. MRI to detect atherosclerosis with gadolinium-containing immunomicelles targeting the macrophage scavenger receptor. Magn Reson Med. 2006;56:601-610.

39. van Tilborg GA, Mulder WJ, Deckers N, Storm G, Reutelingsperger CP, Strijkers GJ, Nicolay K. Annexin A5-functionalized bimodal lipid-based contrast agents for the detection of apoptosis. Bioconjug Chem. 2006;17:741-749.

40. Tsimikas S, Palinski W, Halpern SE, Yeung DW, Curtiss LK, Witztum JL. Radiolabeled MDA2, an oxidation-specific, monoclonal antibody, identifies native atherosclerotic lesions in vivo. J Nucl Cardiol. 1999;6:41-53.

41. Briley-Saebo KC, Shaw PX, Mulder WJ, Choi SH, Vucic E, Aguinaldo JG, Witztum JL, Fuster V, Tsimikas S, Fayad ZA. Targeted molecular probes for imaging atherosclerotic lesions with magnetic resonance using antibodies that recognize oxidation-specific epitopes. Circulation. 2008;117:3206-3215.

42. Briley-Saebo KC, Mulder WJ, Mani V, Hyafil F, Amirbekian V, Aguinaldo JG, Fisher EA, Fayad ZA. Magnetic resonance imaging of vulnerable atherosclerotic plaques: current imaging strategies and molecular imaging probes. J Magn Reson Imaging. 2007;26:460-479.